Neuron, Vol. 46, 205–217, April 21, 2005, Copyright ©2005 by Elsevier Inc. DOI 10.1016/j.neuron.2005.03.019

Vav Family GEFs Link Activated Ephs to Endocytosis and Axon Guidance

Christopher W. Cowan,[1,5] Yu Raymond Shao,[1,2,5] Mustafa Sahin,[1,3] Steven M. Shamah,[1] Michael Z. Lin,[1,2] Paul L. Greer,[1,2] Sizhen Gao,[4] Eric C. Griffith,[1] Joan S. Brugge,[4] and Michael E. Greenberg[1,*]

[1]Neurobiology Program
Children's Hospital and
Departments of Neurology and Neurobiology
Harvard Medical School
300 Longwood Avenue
Boston, Massachusetts 02115

[2]Program in Biological and Biomedical Sciences
Harvard Medical School
240 Longwood Avenue
Boston, Massachusetts 02115

[3]Department of Neurology
Children's Hospital
Boston, Massachusetts 02115

[4]Department of Cell Biology
Harvard Medical School
240 Longwood Avenue
Boston, Massachusetts 02115

Summary

Ephrin signaling through Eph receptor tyrosine kinases can promote attraction or repulsion of axonal growth cones during development. However, the mechanisms that determine whether Eph signaling promotes attraction or repulsion are not known. We show here that the Rho family GEF Vav2 plays a key role in this process. We find that, during axon guidance, ephrin binding to Ephs triggers Vav-dependent endocytosis of the ligand-receptor complex, thus converting an initially adhesive interaction into a repulsive event. In the absence of Vav proteins, ephrin-Eph endocytosis is blocked, leading to defects in growth cone collapse in vitro and significant defects in the ipsilateral retinogeniculate projections in vivo. These findings suggest an important role for Vav family GEFs as regulators of ligand-receptor endocytosis and determinants of repulsive signaling during axon guidance.

Introduction

Eph family receptor tyrosine kinases (Ephs) regulate a wide variety of biological processes in developing and adult organs (Flanagan and Vanderhaeghen, 1998; Kullander and Klein, 2002). Within the nervous system, Eph signaling mediates the initial sorting and positioning of cells and axons during development. Eph signaling regulates the migration pattern of neural crest cells, the boundary formation between hindbrain segments (rhombomeres), the proper formation of the corticospinal tract, and the establishment of visual topographic maps in the midbrain and tectum. Recent studies also indicate that Ephs can regulate the formation and functional properties of neuronal synapses (Henkemeyer et al., 2003; Kullander and Klein, 2002). Thus, Ephs display extensive functional versatility, regulating numerous patterning and morphogenic processes in the developing and mature nervous system.

Much has been learned in recent years about the mechanisms by which Ephs and their ephrin ligands regulate Eph-dependent biological processes. The Ephs (EphA1–8 and EphB1–4,6) are single-pass transmembrane receptors with intrinsic tyrosine kinase activity. Ephrins are membrane tethered as either transmembrane (ephrin-B1–3) or glycosylphosphatidyl inositol-linked (ephrin-A1–5) ligands. Unlike secreted, diffusible guidance cues, such as netrins or slits (Guan and Rao, 2003; Tessier-Lavigne and Goodman, 1996), membrane bound ephrins bind to Ephs only upon cell-cell contact. Ephrin binding to an Eph results in receptor clustering, stimulation of the intrinsic tyrosine kinase activity, and Eph autophosphorylation. This in turn initiates Eph-dependent forward signaling that promotes growth cone attraction or repulsion.

With regard to axonal repulsion, this process has been characterized most thoroughly by studying the effects of soluble ephrin on growth cone dynamics in culture (Drescher et al., 1995; Meima et al., 1997a; Meima et al., 1997b). Under these conditions, ephrin treatment induces a strong repulsion event termed growth cone collapse. Ephrin-induced growth cone collapse requires the activation of RhoA and Rac family of small GTPases (Fournier et al., 2000; Jurney et al., 2002; Wahl et al., 2000). Rac activity is thought to promote internalization of plasma membrane, whereas RhoA activity is critical for promoting contractility and disassembly of the F-actin cytoskeleton. Eph activation of RhoA has been shown recently to be mediated by the Rho family GEF, ephexin1, which in turn regulates growth cone collapse (Shamah et al., 2001; Sahin et al., 2005 [this issue of *Neuron*]). However, the mechanism by which Ephs activate Rac and the role of Rac in mediating Eph-dependent events during development are not yet known.

Axon guidance in vivo involves the cell contact-mediated interaction of membrane bound ephrins and Ephs. The initial interaction between axon growth cone and target cell results in an adhesion between the ephrin and Eph; however, in many cases the contact subsequently promotes repulsion of the axon. Therefore, the Eph-expressing growth cone must overcome ephrin-Eph adhesion if axonal repulsion is to occur. One way in which growth cones may convert the initial ephrin-Eph adhesion into repulsion is by Rac-dependent endocytosis, an atypical endocytic mechanism by which the ephrin-Eph complex and surrounding plasma membrane are internalized into one cell. Two recent studies showed that the endocytosis of the ephrin-Eph complex is required for the repulsion of ephrin-B- and

*Correspondence: michael.greenberg@childrens.harvard.edu

[5]These authors contributed equally to this work.

EphB-expressing cells in culture (Marston et al., 2003; Zimmer et al., 2003). In these experiments, the forward ephrin-Eph endocytosis process requires Eph kinase activity (Marston et al., 2003; Zimmer et al., 2003) and subsequent Rac activity (Marston et al., 2003). Under conditions where ephrin-Eph endocytosis is blocked, the ephrin-Eph interaction results in cell-cell adhesion, suggesting that activation of Rac-dependent endocytosis of the ephrin-Eph complex may convert initial adhesion into repulsive signaling. As such, ephrin-Eph endocytosis may represent a critical point of regulation that determines whether ephrin-Eph binding promotes adhesion/attraction or repulsion. At present, the signaling mechanisms by which ephrin-Eph complexes link to Rac activation and endocytosis are not known, and it is unclear whether ephrin-Eph endocytosis is critical for axon guidance during development.

In this study, we investigated the molecular mechanisms that underlie ephrin-Eph endocytosis and the conversion of ephrin-Eph adhesion into repulsion. We show here that the Rho family GEF Vav2 plays a central role in these processes. In response to ephrin binding to Ephs, Vav2 is recruited to the intracellular domain of Ephs and becomes transiently activated. Vav proteins are required for ephrin-Eph endocytosis and ephrin-induced growth cone collapse, suggesting that Vav GEFs provide a molecular link between activated Ephs and Rac-dependent endocytosis. Analysis of *Vav2*$^{-/-}$ *Vav3*$^{-/-}$ mice revealed abnormal axon projections from the retina to the thalamus, suggesting that Vav GEFs may play an important role in ephrin-Eph endocytosis and Eph-dependent repulsion in vivo. Taken together, these findings suggest that activation of Vav GEFs switches Eph forward signaling from adhesion to repulsion by regulating ephrin-Eph endocytosis. As such, Vav-dependent regulation of receptor endocytosis may determine the biological response to ephrins and possibly other axon guidance factors.

Results

The Rho Family GEF Vav2 Interacts with the Intracellular Domain of EphA4

Using the autophosphorylated intracellular domain of EphA4 (EphA4IC) as bait, we performed a yeast two-hybrid screen with a cDNA library prepared from embryonic day 14 (E14) rat spinal cord and dorsal root ganglia (DRG). In addition to the identification of the RhoA-GEF ephexin1 (Shamah et al., 2001), we isolated the Rho family GEF Vav2 as an EphA4-interacting protein (Figure 1A). Vav2 belongs to a subfamily of GEFs (Vav1, Vav2, and Vav3) that are evolutionarily conserved from nematodes to mammals and play important roles in multiple aspects of cell signaling (Bustelo, 2001; Turner and Billadeau, 2002). To test whether Vav2 interacts with Ephs in mammalian cells, we performed coimmunoprecipitations with full-length versions of Vav2 and EphA4 or EphB2 overexpressed in HEK293T cells. We observed that Vav2 interacted with either EphA4 or EphB2 (Figures 2A and 2B), indicating that Vav2 can bind to either EphA or EphB subclass receptors.

We next asked whether Vav2 might function downstream of Eph forward signaling. In neurons, ephrin binding to an Eph induces receptor clustering and autophosphorylation of the highly conserved juxtamembrane (JM) tyrosines (Y596 and Y602 of EphA4) (Bartley et al., 1994; Davis et al., 1994; Ellis et al., 1996). Eph tyrosine kinase-mediated autophosphorylation of these JM residues generates docking sites for phosphotyrosine binding proteins (Holland et al., 1997; Pandey et al., 1995; Pandey et al., 1994; Stein et al., 1996; Stein et al., 1998; Zisch et al., 1998). Mutant forms of Ephs lacking the intracellular domain or intrinsic kinase activity fail to mediate ephrin-induced axonal repulsion in vitro and in vivo (Dearborn et al., 2002; Kullander et al., 2001; Walkenhorst et al., 2000), suggesting that ephrin binding to Eph induces kinase-dependent forward signaling to promote axonal repulsion. To determine if Vav2 interacts with Ephs in a kinase-dependent manner, we tested whether Vav2 binds to kinase-inactive mutants of EphA4. In both yeast (Figure 1B) and mammalian cells (Figure 2), Vav2 failed to interact with a kinase-inactivated mutant of EphA4 (V635M; Figures 1B and 2C) or with EphA4 JM tyrosine mutants that also lack Eph kinase activity (Y596F, Y602F, or Y596F/Y602F; Figures 1B and 2C and data not shown), suggesting that Vav2 interacts specifically with the ephrin-activated form of the Eph and might play a role in kinase-dependent forward signaling.

The failure of Vav2 to interact with the JM tyrosine

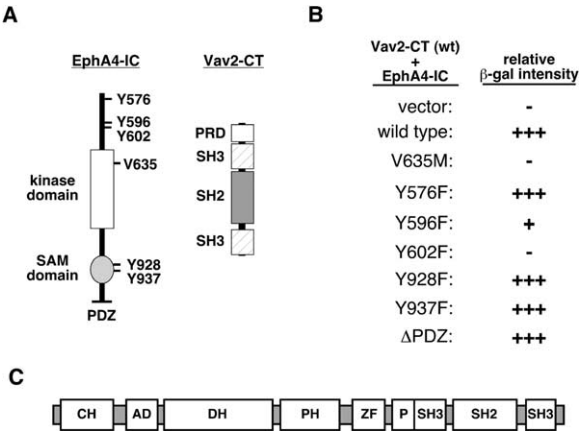

Figure 1. Vav2 Interacts with the Intracellular Domain of EphA4 in the Yeast Two-Hybrid Assay

(A) Domain structures of the intracellular domain of EphA4 (EphA4-IC) bait protein and the interacting clone of Vav2 (Vav2-CT) identified in the yeast two-hybrid screen. SAM domain, sterile α motif domain; PRD, proline-rich domain; SH3, Src homology 3 domain; SH2: Src homology 2 domain.

(B) Characterization of Vav2-CT and EphA4-IC interaction in yeast. Wild-type Vav2-CT was coexpressed in the yeast two-hybrid assay with vector, wild-type, or various mutants of EphA4-IC. V635M, kinase-inactivating mutation; Y576F, Y596F, and Y602F, mutations of juxtamembrane tyrosines; Y928F and Y937F, mutations of tyrosine residues in SAM domain; ΔPDZ, deletion of PDZ binding motif.

(C) Domain composition of Vav family proteins, adapted from Turner and Billadeau (2002). CH, calponin homology domain; AD, acidic domain; DH, Dbl homology domain; PH, pleckstrin homology domain; ZF, zinc finger domain; P, proline-rich domain; SH3, Src homology type 3 domain; SH2, Src homology type 2 domain.

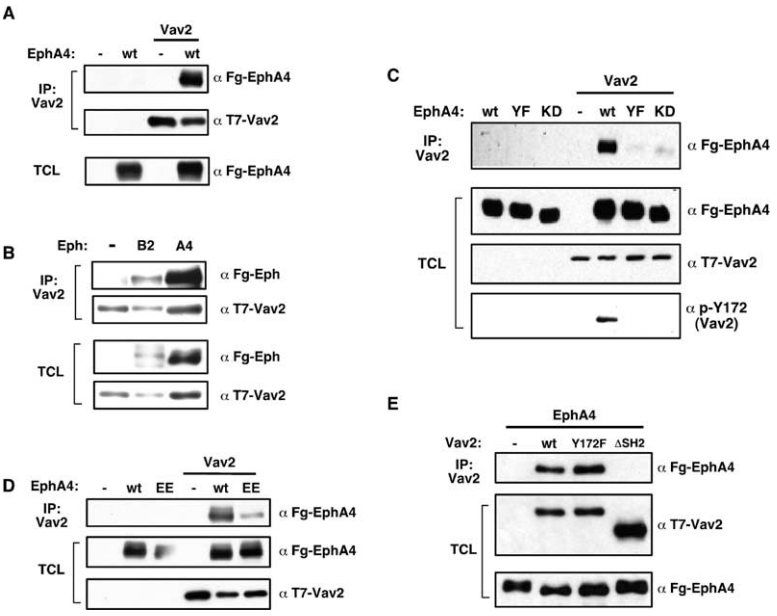

Figure 2. Vav2 and Ephs Interact in Mammalian Cells

(A and B) Coimmunoprecipitation of Vav2 and EphA4 or EphB2 in HEK293T cells. Cells were transfected with T7-tagged Vav2 and Flag-tagged EphA4 or EphB2. Total cell lysates (250 μg) were immunoprecipitated with anti-T7 antibody, then immunoblotted with anti-Flag (Eph) or anti-T7 (Vav2) antibodies. Whole-cell lysates (12.5 μg) were also blotted with anti-Flag or anti-T7 antibody.

(C–E) Analysis of the Vav2 and EphA4 interaction by coimmunoprecipitation. (C) T7-tagged Vav2 was coexpressed with Flag-tagged EphA4 (wt), EphA4-YF (Y602F), or EphA4-KD (kinase dead: V635M); (D) T7-tagged Vav2 was coexpressed with Flag-tagged EphA4 (wt) or a JM tyrosine mutant of EphA4 (EE: Y596E/Y602E); (E) Flag-tagged EphA4 was coexpressed with T7-tagged Vav2 (wt), Vav2-Y172F, or ΔSH2-Vav2. Total cell lysates (TCL) were blotted with anti-Flag, anti-T7, or a p-Y172-specific Vav2 antibody. The autoradiograph exposures shown were chosen to illustrate relative loading and protein expression levels rather than to indicate the degree of immunoprecipitation or coimmunoprecipitation from the cell lysates.

mutants of EphA4 suggests a possible direct interaction with the phosphorylated JM tyrosines; however, previous studies have shown that tyrosine to phenylalanine mutation of the JM tyrosines also leads to a loss of Eph kinase activity (Binns et al., 2000; Zisch et al., 1998; Zisch et al., 2000). To test whether Vav2 directly binds to the JM tyrosines, we tested the ability of Vav2 to bind to a mutant of EphA4 (Y596E/Y602E) that retains normal tyrosine kinase activity but cannot be phosphorylated at the JM tyrosines (Zisch et al., 2000). We found that Vav2 interacted much more weakly with the YE mutant than wild-type EphA4, suggesting that Vav2 interacts directly with phosphorylated JM tyrosines of EphA4 (Figure 2D). The residual binding of Vav2 to the YE mutant may be mediated by the negative charge of the glutamic acid (E), a substitution that is often used to mimic phosphorylation. These findings suggest that, upon ephrin binding to an Eph, the Eph autophosphorylation of the JM tyrosines generates a docking site for Vav2 recruitment.

How then does Vav2 interact with the phosphorylated JM tyrosines? All the Vav family GEFs contain a SH2 phosphotyrosine binding domain in the C-terminal portion of the protein. Therefore, we speculated that Vav2 might be recruited to the phosphorylated JM tyrosines of ephrin-activated Ephs via its SH2 domain. We tested the ability of Vav2 containing a mutated SH2 domain (ΔSH2-Vav2) to interact with wild-type EphA4. We found that, in contrast to wild-type Vav2, ΔSH2-Vav2 does not interact with EphA4 (Figure 2E). We conclude that, once ephrin activates Eph and the JM tyrosines become autophosphorylated, Vav2 is recruited to the ephrin-Eph complex and binds to Eph JM tyrosines via the Vav2 SH2 domain.

Having established that Vav2 and Ephs interact in a phosphorylation-dependent manner, we sought to determine whether activated Ephs might regulate the GEF activity of Vav2. A combination of biochemical, mutational, and structural data indicate that phosphorylation of conserved tyrosine residues in the acidic domain of Vavs regulates the GDP/GTP exchange activity of Vav proteins (Aghazadeh et al., 2000; Crespo et al., 1997; Lopez-Lago et al., 2000; Movilla and Bustelo, 1999; Schuebel et al., 1998). In the absence of tyrosine phosphorylation, an intramolecular interaction of the Vav acidic domain with the catalytic Dbl homology (DH) domain blocks access to Rho family GTPases. This inhibitory interaction is disrupted when Vav is phosphorylated at highly conserved tyrosines in the acidic domain (e.g., Tyr174), resulting in active GDP/GTP exchange on Rho family GTPases. As an activating mutation of Tyr174 on Vav1 has previously been shown to be sufficient to induce near maximal GDP exchange activity, we utilized a site-specific phospho-antibody against this site on Vav2 (Tyr172) to determine if activated EphA4 induces tyrosine phosphorylation of this regulatory site on Vav2. While little tyrosine phosphorylation of Vav2 was detected in the absence of EphA4 expression, coexpression in HEK293T cells of Vav2 and wild-type EphA4 significantly increased Vav2 Tyr172 phosphorylation (Figure 2C). As with EphA4, the coexpression of EphA7, EphB2, EphB3, or EphB4 with Vav2 led to significant Tyr172 phosphorylation (data not shown), suggesting that multiple EphAs and EphBs are capable of activating Vav2. However, it was unclear whether enhanced phosphorylation of Vav2 was dependent on a physical association between the Vav2 and Eph or due to an indirect Eph-dependent signaling event. Coexpression of wild-type EphA4 with the ΔSH2-Vav2 mutant that failed to interact with the activated

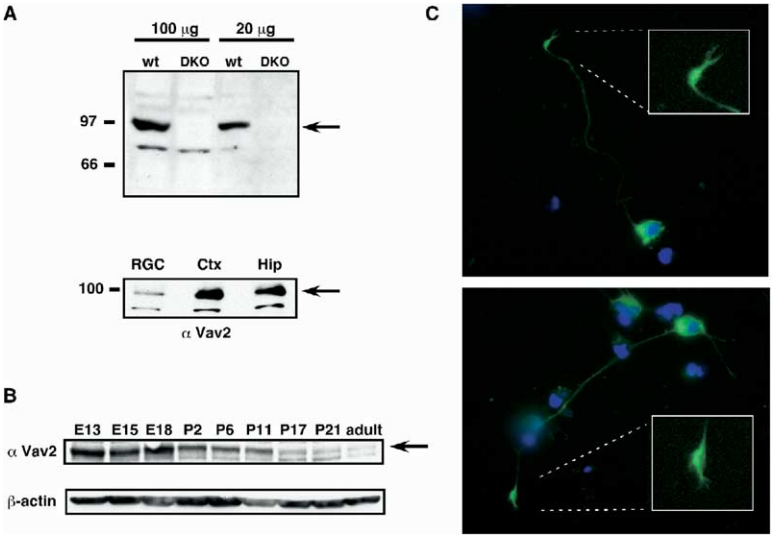

Figure 3. Vav2 Protein Expression in Neurons

(A) Western blotting with Vav2 antibodies in whole-brain lysates from wild-type or *Vav2*$^{-/-}$ *Vav3*$^{-/-}$ mice, or from dissociated primary rat neurons. Lysates represent total protein from 150,000 rat P6 retinal ganglion cells, 750,000 rat E17/18 cortical neurons, or 750,000 rat E17/18 hippocampal neurons.

(B) Developmental expression profile of Vav2 or β-actin from whole-brain lysates (no cerebellum) at indicated embryonic (E) or postnatal (P) day (100 μg/lane).

(C) Expression of Vav2-EGFP (green) or nuclear staining (Hoechst, blue) in E17/18 cortical neurons at 3 days in culture (inset, growth cone region of Vav2-EGFP-expressing neurons).

EphA4 did not result in Vav2 tyrosine phosphorylation at Tyr172 (data not shown), indicating that Vav2 tyrosine phosphorylation and activation require a direct interaction of Vav2 with the activated Eph. Similarly, coexpression of the EphA4 YE mutant with Vav2 resulted in decreased levels of binding (Figure 2D) as well as decreased levels of Vav2 tyrosine phosphorylation (data not shown). We note that phosphorylation of Vav2 on Tyr172 was not necessary for binding to EphA4 (Figure 2E), suggesting that Vav2 phosphorylation is a consequence of the interaction with EphA4, not the cause. Taken together, these experiments suggest that, when Ephs become tyrosine autophosphorylated, the activated Eph interacts with Vav2 and triggers Vav2 tyrosine phosphorylation and activation.

Endogenous Vav2 Is Transiently Activated by Ephrin Stimulation in Neurons

Having established that Vav2 binds to and is activated by Ephs, we sought to address three major questions: (1) is Vav2 expressed in neurons, (2) is Vav2 found in growth cones where Eph-dependent axon guidance occurs, and (3) does ephrin stimulation of endogenous Eph receptors induce the activation of Vav2? To determine if Vav2 is expressed in neurons, we tested total brain and primary neuronal culture lysates by Western blotting with an anti-Vav2 antibody. We detected an ~95 kDa band that comigrates with recombinant Vav2 and is absent in adult brain lysates obtained from *Vav2*$^{-/-}$*Vav3*$^{-/-}$ mice, suggesting that the 95 kDa band is a Vav family member (Figure 3A). By Western blotting, Vav2 was also detected in lysates from E17/18 cultured rat cortical, striatal, or hippocampal neurons, as well as rat and mouse RGCs isolated from postnatal day 6 (P6) retinas (Figure 3A and data not shown). We conclude that Vav2 is expressed in a variety of embryonic and postnatal neurons. To determine whether Vav2 is expressed at an appropriate time to play a role in axon guidance, we isolated rat brains over a wide range of embryonic and postnatal days during development (E13 to adult) and analyzed Vav2 protein expression by Western blotting. We found that Vav2 protein is expressed most highly during embryonic (E13–E18) and early postnatal time points (P2–P6) but then declines postnatally when synaptic proteins such as PSD-95 are being upregulated (Figure 3B and data not shown). Therefore, Vav2 protein is expressed highly in the brain during the period when axon guidance is occurring in vivo.

To determine whether Vav2 is found in growth cones, we used several different approaches. As our anti-Vav2 antibodies failed to show specific staining in cultured wild-type neurons, we analyzed the localization of a Vav2-EGFP fusion protein in cultured cortical and hippocampal neurons (Figure 3C and data not shown). We detected Vav2-EGFP in growth cones (Figure 3C, inset), neurites, and the cell body, but not the nucleus, consistent with previous reports of neuronal Vav2 localization (Chauvet et al., 2003). To analyze Vav2 protein subcellular distribution a different way, we harvested distal axons or cell bodies from rat DRG explants grown in compartmentalized chambers. By Western blotting, Vav2 was detected in both distal axons and cell bodies, although Vav2 was found to be most abundant in the cell body fraction. In contrast, the nuclear proteins CBP and MECP2 were detected in the cell body fraction, but not in the distal neurites (data not shown). Thus, Vav2 is present in a number of ephrin-responsive neurons, is synthesized in the brain during the time when axon guidance is occurring, and is detected in the growth cones and distal neurites where ephrin-induced axon guidance occurs.

Finally, we asked if Vav2 becomes tyrosine phosphorylated by ephrin binding to Ephs in neurons. To this end, primary rat cortical or striatal cultures were treated with ephrin-A1 to specifically activate EphAs, ephrin-B1 to selectively stimulate EphBs, or an Fc control protein. Cells were harvested at various times following stimulation, and Vav2 was immunoprecipitated. The activation state of Vav2 was assessed by Western blotting using a general anti-phosphotyrosine monoclonal antibody (4G10) or the anti-Vav2 p-Tyr172 site-specific antibody. Upon ephrin-A1 stimulation, Vav2 became phosphorylated rapidly and transiently, with Vav2 phos-

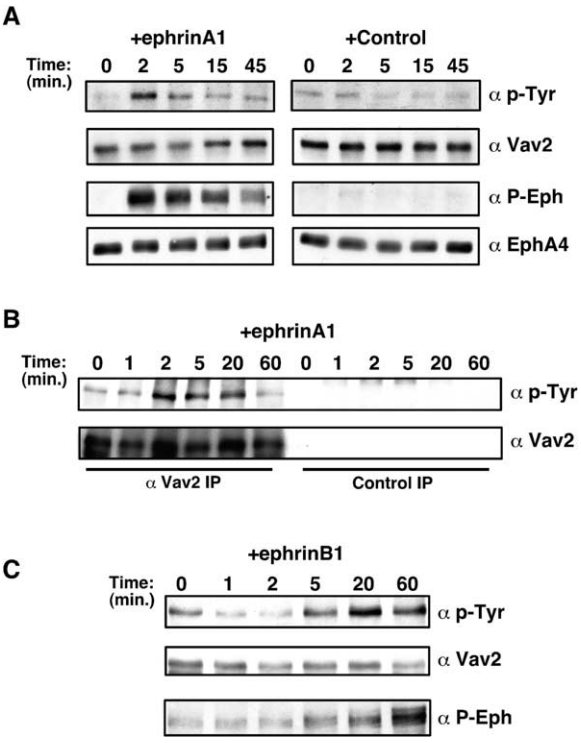

Figure 4. Ephrin Stimulation Activates Endogenous Vav2 in Neurons

(A) E17/18 cortical neurons were cultured for 4 days and then stimulated with ephrin-A1-Fc or Fc (control) for the indicated times. Vav2 was immunoprecipitated from whole-cell lysates and then blotted with phosphotyrosine antibody (4G10) (top panel) or the p-Y172-specific Vav2 antibody (data not shown). Whole-cell lysates were also blotted with anti-Vav2, anti-phospho-Eph, or anti-EphA4 antibodies.

(B) E17/18 striatal neurons cultured for 4 days were stimulated with 5 μg/ml clustered ephrin-A1-Fc. Cell lysates were immunoprecipitated with anti-Vav2 antibody or Protein A beads alone (control IP) and blotted with anti-phosphotyrosine antibody or anti-Vav2 antibody.

(C) Cortical neurons at E17/18 + 4 DIV were stimulated with ephrin-B1-Fc. Vav2 was immunoprecipitated and blotted with phosphotyrosine antibody. Total cell lysates were blotted with anti-Vav2 or site-specific antibodies against the phosphorylated JM tyrosines of Ephs.

phorylation detectable as early as 1 min following stimulation with ephrin-A1 (Figures 4A and 4B). The peak of Vav2 phosphorylation was between 2 and 5 min, and then Vav2 phosphorylation declined quickly thereafter. Similarly, ephrin-B1 stimulation induced the transient phosphorylation of Vav2, but with delayed kinetics that mirrored the activation phase of the EphBs (Figure 4C). Treatment with Fc control did not induce Vav2 tyrosine phosphorylation at any of the time points analyzed. Taken together, these experiments suggest that Vav2 is transiently tyrosine phosphorylated and activated in neurons by Eph forward signaling under conditions that induce Eph-dependent repulsion.

Abnormal Retinogeniculate Projections in the *Vav2*$^{-/-}$*Vav3*$^{-/-}$ Mice

Since ephrin/Eph forward signaling induces the transient phosphorylation of Vav2 in neurons, and Ephs are known to be critical for proper axon guidance during development, we investigated whether Vav proteins might also be necessary for proper axon guidance in vivo. Since Vav2 and Vav3 are known to be expressed in the brain, are closely related with respect to amino acid sequence, and are both activated by tyrosine phosphorylation (Movilla and Bustelo, 1999; Schuebel et al., 1998), we speculated that a potential role for Vav2 or Vav3 in Eph-dependent signaling might be unclear in the single knockout mice due to compensation by the remaining Vav gene product. Therefore, we analyzed the projection pattern of axons from retinal ganglion cells (RGCs) to the dorsal lateral geniculate nucleus (dLGN) in wild-type and *Vav2*$^{-/-}$*Vav3*$^{-/-}$ mice. To visualize Eph-dependent axon projections, we injected the left and right eyes with either Alexa 488 (green)- or Alexa 594 (red)-conjugated cholera toxin B (ChTxB) subunits to anterogradely label the axon terminals in the dLGN. As shown in Figure 5A, the wild-type contralateral projections (green) occupy a large majority of the dLGN, whereas the ipsilateral projections (red) occupy a smaller, centrally located, and spatially segregated region of the dLGN. By casual observation, the ipsilateral projections in *Vav2*$^{-/-}$*Vav3*$^{-/-}$ mice appear to be reduced in number and ventrally shifted, and to display a patchy pattern when compared to wild-type animals.

To analyze ipsilaterally projecting axons more carefully, we quantified the total signal intensity and average distribution for all ipsilateral projections to the dLGN in both wild-type and *Vav2*$^{-/-}$*Vav3*$^{-/-}$ mice. By these analyses (Figure 5C, top), we observed a 55% decrease in the total ipsilateral projection signal in the *Vav2*$^{-/-}$*Vav3*$^{-/-}$ mice as compared to wild-type mice, indicating that *Vav2*$^{-/-}$*Vav3*$^{-/-}$ mice have fewer total ipsilateral projections. As this reduction could be due to reduced labeling efficiency in the eye or reduced transport of the anterograde label to the nerve terminals of *Vav2*$^{-/-}$*Vav3*$^{-/-}$ mice, we analyzed the contralateral projections to determine if there was a similar decrease in signal intensity in *Vav2*$^{-/-}$*Vav3*$^{-/-}$ mice. However, we found that the total signal intensity of *Vav2*$^{-/-}$*Vav3*$^{-/-}$ contralateral projections was similar to that of the wild-type mice (Figure 5C, bottom), indicating that the significant decrease in the number of ipsilateral projections to the *Vav2*$^{-/-}$*Vav3*$^{-/-}$ dLGN is not due to an overall decrease in labeling efficiency or to lower levels of ChTxnB at dLGN nerve terminals.

The number of ipsilateral projections in mutant and wild-type dLGNs was also quantified by generating binary images of ipsilateral and contralateral projections to the dLGN (Figure 5B). By this method of analysis, we also detected a decrease in the number of ipsilateral projections in *Vav2*$^{-/-}$*Vav3*$^{-/-}$ mice relative to wild-type mice (data not shown). By contrast, pixel occupancy for the contralateral projections was similar in *Vav2*$^{-/-}$*Vav3*$^{-/-}$ and wild-type animals. The decrease in ipsilateral projections in the *Vav2*$^{-/-}$*Vav3*$^{-/-}$ mice is similar in magnitude to the reduction in ipsilateral projections observed in the *EphB1*$^{-/-}$ and *EphB1*$^{-/-}$*EphB2*$^{-/-}$*EphB3*$^{-/-}$ mice (Williams et al., 2003). The finding that there is a reduction in ipsilateral axon projections in Vav-deficient mice indicates that Vav proteins are important for proper axon targeting to the dLGN and raises the possibility that Ephs promote axon guidance via a Vav- and Rac-dependent process.

In addition to the reduction of ipsilateral nerve ter-

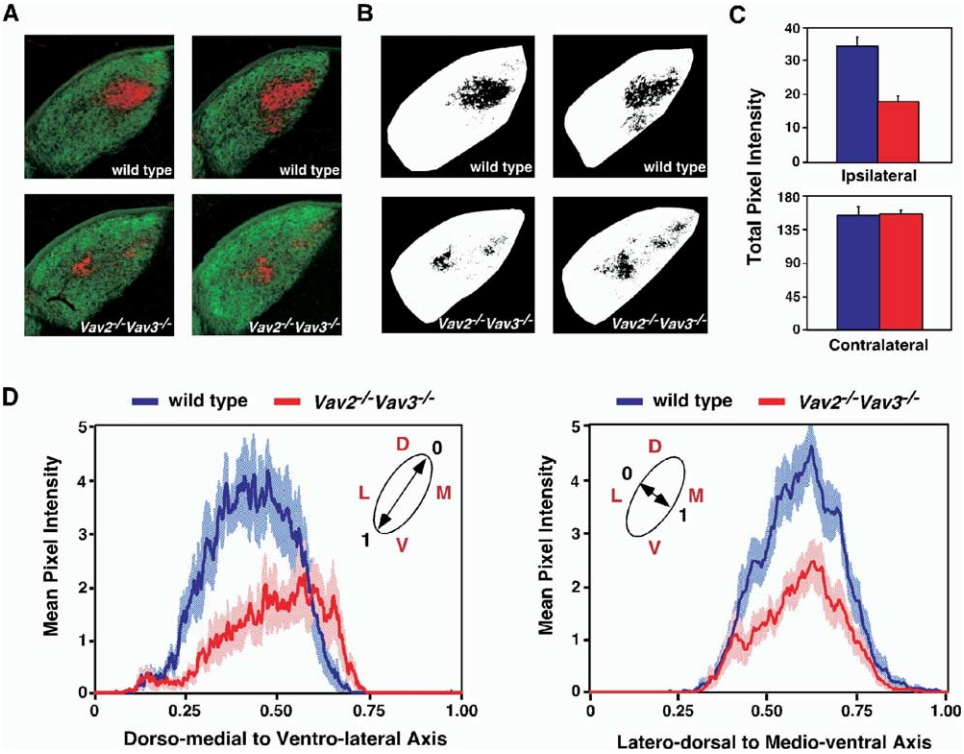

Figure 5. Retinogeniculate Projections Are Altered in the *Vav2*$^{-/-}$*Vav3*$^{-/-}$ Mice

(A) Confocal images of contralateral (green) and ipsilateral (red) axon projections in the dorsal lateral geniculate nucleus (dLGN) from two wild-type (top) and two *Vav2*$^{-/-}$*Vav3*$^{-/-}$ (bottom) mice.

(B) Corresponding binary images of the ipsilateral projections from the wild-type (top) and *Vav2*$^{-/-}$*Vav3*$^{-/-}$ (bottom) mice.

(C) Analysis of the total axon projections (ipsilateral and contralateral) between wild-type (blue) and *Vav2*$^{-/-}$*Vav3*$^{-/-}$ (red) mice. Data represent the mean of 11 wild-type and 12 *Vav2*$^{-/-}$*Vav3*$^{-/-}$ mice ± SEM. The difference of total ipsilateral projections ([C], top) between the wild-type and Vav mutant mice is statistically significant (Student's t test; $p < 0.001$).

(D) Average distribution (mean ± SEM) of the ipsilateral projections along the long (dorsomedial to ventrolateral) and short (laterodorsal to medioventral) axes. The data are plotted on a normalized axis (0 to 1) of the long and short axis of the dLGN as depicted on the inset diagrams. D, dorsal; V, ventral; L, lateral; M, medial.

minals in the *Vav2*$^{-/-}$*Vav3*$^{-/-}$ mice, the distribution of ipsilateral projections appears to be more diffuse, patchy, and skewed toward the ventrolateral region of the dLGN (Figures 5B and 5D). To compare the distribution of the ipsilateral projection pattern, we employed a line scan technique to calculate the mean pixel intensity of projection terminals in wild-type and *Vav2*$^{-/-}$*Vav3*$^{-/-}$ mice along the long (dorsomedial [DM] to ventrolateral [VL]) and short (laterodorsal [LD] to medioventral [MV]) axes. The mean pixel intensity for each pixel line was averaged for 11 wild-type mice (blue line, Figure 5D) and 12 *Vav2*$^{-/-}$*Vav3*$^{-/-}$ mice (red line, Figure 5D). The distribution of axon projections along the short axis (Figure 5D, right panel) appeared similar in wild-type and *Vav2*$^{-/-}$*Vav3*$^{-/-}$ mice, indicating that Vav proteins are dispensable for proper axon targeting along this axis. However, the distribution of projections along the long axis, which coincides with the orientation of the ephrin-A gradient in wild-type mice, was distorted in the *Vav2*$^{-/-}$*Vav3*$^{-/-}$ mice (Figure 5D, left panel). Wild-type mice displayed a bell-shaped distribution of projections, with the center of the distribution just dorsal to the midline. In contrast, the *Vav2*$^{-/-}$*Vav3*$^{-/-}$ mice showed a distinct VL-shifted and sloping distribution, indicating that the ipsilateral axons in the *Vav2*$^{-/-}$*Vav3*$^{-/-}$ mice that successfully project to the dLGN are abnormal in their targeting. This ventrolateral skewing of ipsilateral projections in Vav-deficient animals may be the result of a defect in Eph signaling. Taken together, the projection defects in the *Vav2*$^{-/-}$*Vav3*$^{-/-}$ mice indicate an important role for Vav family GEFs in the proper formation of the ipsilateral retinogeniculate map and raise the possibility that Vav proteins may regulate aspects of ephrin/Eph-dependent axon guidance.

Vav Family GEFs Are Necessary for Ephrin-Induced Growth Cone Collapse of RGCs

Axonal repulsion in vivo requires an initial adhesive interaction between ephrins expressed on target cells and Ephs expressed on guiding axonal growth cones. Subsequent to ephrin-Eph binding, the Ephs cluster and autophosphorylate their JM tyrosines, which in turn stimulate signaling events that switch from adhesion to repulsion. One possible reason for abnormal Eph-mediated axon guidance in the Vav-deficient mice might be a defect in the initial ephrin-Eph adhesion event. To address this possibility, we cultured dissociated RGCs from wild-type and Vav-deficient mice and

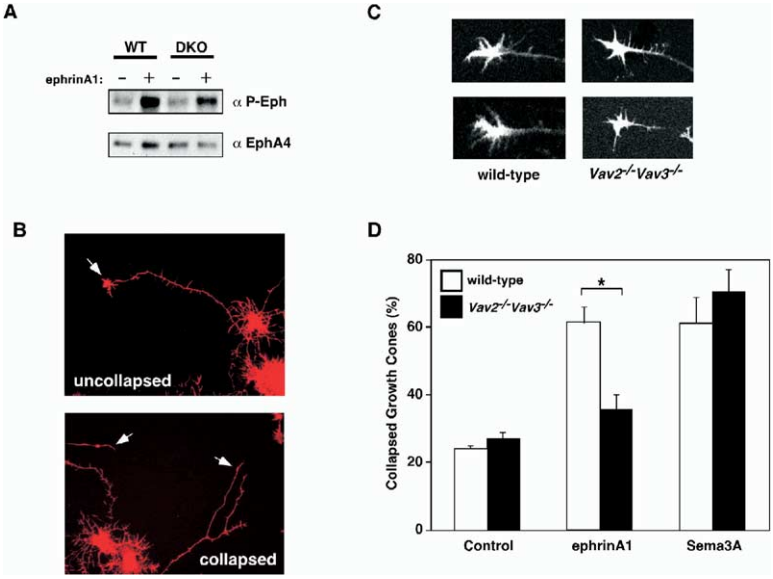

Figure 6. Vav Family GEFs Are Necessary for Ephrin-A1-Induced Growth Cone Collapse of Retinal Ganglion Cells

(A) Cultured wild-type and *Vav2*$^{-/-}$*Vav3*$^{-/-}$ retinal ganglion cells (RGCs) were stimulated with clustered ephrin-A1 or Fc control for 12 min, and then lysates were immunoblotted with anti-phospho-Eph (top) or anti-EphA4-specific (bottom) antibodies.

(B) Morphology of uncollapsed (top) and collapsed (bottom) growth cones were visualized with Texas red-labeled phalloidin (Molecular Probes).

(C) F-actin content and growth cone morphology of wild-type (left) and *Vav2*$^{-/-}$*Vav3*$^{-/-}$ (right) RGCs (phalloidin-Texas red).

(D) Growth cone collapse assay with wild-type (open bars) and *Vav2*$^{-/-}$*Vav3*$^{-/-}$ (closed bars) RGCs. Cultured RGCs (P7, 2 DIV) were stimulated with ephrin-A1, Semaphorin 3A (Sema3A), or Fc control for 30 min prior to fixation and phalloidin staining. Data represent the mean of three (Sema3A) or four (ephrin-A1 and Fc) independent experiments ± SEM. Asterisk marks significant difference between wild-type and mutant RGCs (Student's t test; p = 0.001).

incubated them with ephrin-A1-Fc or Fc at 4°C in order to detect ephrin-Eph surface binding. We detected a similar staining intensity and signal distribution of surface bound ephrin (data not shown), indicating that ephrin-Eph adhesion is normal in the RGCs of *Vav2*$^{-/-}$ *Vav3*$^{-/-}$ mice. We next asked whether Eph activation by tyrosine autophosphorylation might be defective in the *Vav2*$^{-/-}$*Vav3*$^{-/-}$ mice, thus resulting in defective Eph forward signaling. However, stimulation of cultured RGCs from either wild-type or *Vav2*$^{-/-}$*Vav3*$^{-/-}$ mice with ephrin-A1 led to a significant increase in JM tyrosine autophosphorylation (Figure 6A), suggesting that axon guidance defects in Vav-deficient mice are not likely due to abnormal ephrin-Eph adhesion or initial receptor activation.

To investigate whether the axon guidance defects observed in the *Vav2*$^{-/-}$*Vav3*$^{-/-}$ mice might be due to defects in Eph-dependent repulsion signaling, we turned to a neuronal culture-based assay. Addition of ephrin-As to dissociated RGCs in culture induces a dramatic change in the morphology of axonal growth cones that is characterized by the retraction of extending filopodia and the collapse of the growth cone (Figure 6B). To determine if Vav family GEFs are required for ephrin-induced growth cone collapse, we examined the response of RGCs derived from wild-type and *Vav2*$^{-/-}$*Vav3*$^{-/-}$ mice to ephrin-A1 stimulation. Importantly, the overall cell morphology, number of neurites, and growth cone morphology of cultured *Vav2*$^{-/-}$*Vav3*$^{-/-}$ RGCs appeared similar to wild-type RGCs (Figure 6C). After 2 days in culture, RGCs were stimulated with ephrin-A1 or Fc control for 30 min, then fixed and scored for collapsed or uncollapsed growth cones. Ephrin-A1 treatment induced the collapse of a large percentage of the growth cones in wild-type RGC cultures as compared to the Fc control treatment (61% and 24%, respectively; Figure 6D, open bars). In contrast, *Vav2*$^{-/-}$*Vav3*$^{-/-}$ RGCs were poorly responsive to ephrin-A1 treatment when compared to the Fc control (36% and 28%, respectively; Figure 6D, solid bars). Thus, Vav family GEFs play a key role in mediating ephrin-dependent growth cone collapse.

The observation that there is a defect in ephrin-induced growth cone collapse of Vav-deficient RGCs suggests that there is a specific deficit in Eph signaling in these cells. However, we considered the alternative possibility that *Vav2*$^{-/-}$*Vav3*$^{-/-}$ RGCs might have an intrinsic defect in the ability to respond to many repulsive guidance factors. To address this possibility, we compared the response of wild-type and *Vav2*$^{-/-}$*Vav3*$^{-/-}$ RGCs to treatment with Semaphorin 3A (Sema3A), a secreted ligand that stimulates growth cone collapse through the neuropilin1/plexin-A1 receptor complex (He and Tessier-Lavigne, 1997; Kolodkin et al., 1997; Kolodkin et al., 1992; Luo et al., 1993; Takahashi et al., 1999; Tamagnone et al., 1999). We detected no significant difference in Sema3A-induced growth cone collapse between wild-type and *Vav2*$^{-/-}$*Vav3*$^{-/-}$ RGCs (Figure 6D). Taken together, these findings indicate that the growth cone collapse deficit in *Vav2*$^{-/-}$*Vav3*$^{-/-}$ RGCs reflects a specific defect in Eph-dependent signaling.

Vav Family GEFs Are Required for Ephrin-Eph Endocytosis

We next explored the cellular mechanism by which Vav proteins regulate ephrin-Eph-mediated growth cone collapse. Vav proteins have been shown to activate RhoA, Rac, and Cdc42 proteins in vitro. However, studies of Vav proteins in mammalian cells have revealed that they induce membrane ruffles and lamellipodia and strongly activate Rac family GTPases (Arthur et al., 2004; Kawakatsu et al., 2005; Liu and Burridge, 2000; Marcoux and Vuori, 2003; Marignani and Carpenter, 2001; Schuebel et al., 1998; Servitja et al., 2003; Tamas et al., 2003). Since Rac activity has been shown to be required for ephrin-Eph endocytosis (Marston et

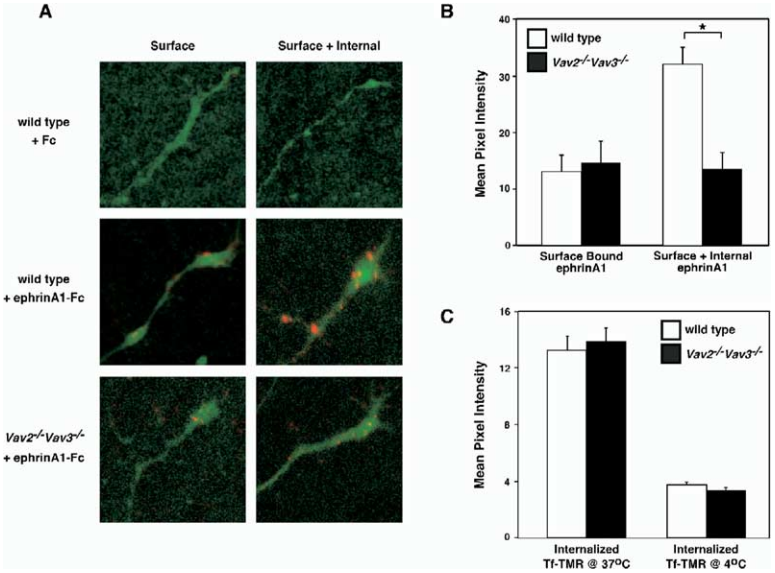

Figure 7. Vav Family GEFs Are Required for Ephrin-Eph Endocytosis

(A) Fluorescence images of Fc control or ephrin-A1-Fc staining (red) of wild-type or *Vav2*$^{-/-}$*Vav3*$^{-/-}$ RGC distal neurites/growth cones (green, DiO). "Surface" represents RGCs blocked without 0.1% Triton X-100, whereas "surface plus internal" represents RGCs blocked in the presence of 0.1% Triton X-100.

(B) Quantification of ephrin-A1 staining intensity of nonpermeabilized or detergent-permeabilized RGC distal neurite/growth cones from wild-type (open bars) and *Vav2*$^{-/-}$ *Vav3*$^{-/-}$ (closed bars) mice after 30 min of stimulation (see Experimental Procedures). The difference between the nonpermeabilized and permeabilized levels indicates the internalized fraction of ephrin-A1. Data represent intensity quantification of a total of 25 to 47 growth cones for each condition from three independent experiments ± SEM. The amount of internalized ephrin-A1 in *Vav2*$^{-/-}$*Vav3*$^{-/-}$ RGCs was significantly different than that of wild-type neurons (ANOVA test; $p < 0.001$).

(C) The endocytosis of transferrin by wild-type (open bars) and *Vav2*$^{-/-}$*Vav3*$^{-/-}$ (closed bars) RGCs was determined following a 30 min incubation with TRITC-labeled transferrin at 37°C (endocytosis permissive) or 4°C (endocytosis blocked). Internalized transferrin was quantified after acid/high-salt wash to remove surface bound ligand. Data represent a total of 32 to 36 neurons for each condition ± SEM.

al., 2003), we investigated the possibility that Vav-deficient RGCs might be defective in ephrin-Eph endocytosis. We compared the internalization of ephrin-A1/EphA complexes in growth cones of cultured RGCs from wild-type and *Vav2*$^{-/-}$*Vav3*$^{-/-}$ mice (Figure 7). Briefly, RGC cultures were treated with ephrin-A1-Fc or Fc control, then fixed and stained to detect the amount of endocytosed ephrin-A1. Total ephrin-A1 staining (surface bound + internalized) was determined under detergent permeabilizing conditions, whereas surface bound ephrin-A1 was specifically measured under nonpermeabilizing conditions. The endocytosed fraction of ephrin-A1 represents the difference between the total staining and the surface bound staining. In wild-type mouse and rat RGCs, the amount of endocytosed ephrin-A1 increased in a time-dependent manner (data not shown). In contrast, no significant ephrin-Eph endocytosis was observed in the Vav-deficient RGCs when compared with wild-type cells at any time tested (Figure 7B and data not shown). For both wild-type and *Vav2*$^{-/-}$*Vav3*$^{-/-}$ RGC cultures, the incubation with Fc control or no treatment failed to induce detectable endocytosis (Figure 7A). Thus, Vav family proteins are necessary for internalization of the ephrin-Eph complex, suggesting that the failure of Vav-deficient RGC growth cones to collapse in response to ephrin treatment may be due, at least in part, to defective ephrin-Eph endocytosis.

To determine whether *Vav2*$^{-/-}$*Vav3*$^{-/-}$ RGCs were generally defective in receptor-dependent endocytosis or whether the internalization defect was specific for ephrin-Eph complexes, we analyzed the endocytosis of transferrin in wild-type and *Vav2*$^{-/-}$*Vav3*$^{-/-}$ neurons. Transferrin is a serum protein that delivers bound iron atoms to the intracellular compartment of cells by constitutive receptor-mediated endocytosis. Using fluorescently labeled transferrin protein, we detected a similar amount of endocytosis in cultured RGCs derived from wild-type or *Vav2*$^{-/-}$*Vav3*$^{-/-}$ mice (Figure 7C), suggesting that Vav proteins are required for endocytosis of the ephrin-Eph complex, but not all endocytic processes. Taken together, our observations that there are defects in ephrin-induced growth cone collapse and ephrin-Eph endocytosis in Vav-deficient RGCs suggest that defects in axon guidance observed in *Vav2*$^{-/-}$*Vav3*$^{-/-}$ mice might be due, at least in part, to a defect in endocytosis-dependent Eph repulsive signaling.

Discussion

In this study, we show that when ephrins bind to Ephs the Rho family GEF, Vav2, is recruited to the phosphorylated JM region of activated Ephs, and Vav2 becomes transiently phosphorylated on tyrosine residues that stimulate its GEF activity. We observed retinogeniculate axonal projection defects in the *Vav2*$^{-/-}$*Vav3*$^{-/-}$ mice, indicating an important role for Vav proteins in neuronal development and suggesting a possible role for Vav proteins in Eph-dependent axonal targeting in vivo. We find that RGCs derived from *Vav2*$^{-/-}$*Vav3*$^{-/-}$ mice fail to collapse their growth cones in response to ephrin-A stimulation in culture. In addition, Vav proteins are necessary for ephrin-Eph endocytosis, a Rac-dependent process that appears to be important for the process of axonal repulsion. Taken together, our data suggest that defects in Vav-dependent Eph signaling result in axon targeting defects in vivo and that Vav proteins promote the local and transient activation of a Rho family GTPase to stimulate ephrin-Eph endocytosis, an important early step in axonal repulsion.

As with any complex mouse phenotype, it is difficult to link definitively the retinogeniculate defects in the

Vav2$^{-/-}$*Vav3*$^{-/-}$ mice to a specific signaling pathway. While our data suggest that the retinogeniculate map defects in the *Vav2*$^{-/-}$*Vav3*$^{-/-}$ mice may be due to disrupted Vav-dependent Eph repulsive signaling, it is important to note that Vav proteins are activated downstream of several growth factor receptors, immune cell receptors, and adhesion molecules (Bustelo, 2000). Defective signaling downstream of one or several of these various receptors could contribute to the disruption of the retinogeniculate projection map in a number of ways. These include effects on axon outgrowth, neurite pruning/branching, or gene expression. With regard to axon outgrowth, we find that in culture the neurites from wild-type and *Vav2*$^{-/-}$*Vav3*$^{-/-}$ RGCs are similar in length (C.W.C., unpublished data). In addition, axon projections to the contralateral dLGN in the *Vav2*$^{-/-}$ *Vav3*$^{-/-}$ mice appear normal (Figure 5C, bottom), suggesting that there is not a general defect in axon outgrowth. We have also considered the possibility that the altered retinogeniculate projections in *Vav2*$^{-/-}$ *Vav3*$^{-/-}$ mice could be due to changes in ephrin or Eph expression levels. To begin to address this possibility, we analyzed by semiquantitative RT-PCR the levels of several ephrin and Eph mRNAs in the brain and eye of wild-type and *Vav2*$^{-/-}$*Vav3*$^{-/-}$ mice. We observed no obvious differences between wild-type and *Vav2*$^{-/-}$ *Vav3*$^{-/-}$ mice in the mRNA levels of ephrins and Ephs that are known to contribute to retinogeniculate or retinocollicular axon targeting (Figure S1 in the Supplemental Data available with this article online).

If Vav-dependent endocytosis is required for Eph repulsive signaling during neuronal development, it is important to consider how disruption of Vav-dependent Eph signaling might cause defects in axon guidance. Recent studies are consistent with the possibility that the observed reduction in ipsilateral projections in the *Vav2*$^{-/-}$*Vav3*$^{-/-}$ mice might be due in part to failure of the ipsilateral axons to repel at the optic chiasm. Specifically, wild-type RGC axons arriving at the optic chiasm encounter ephrin-B2-expressing glia. EphB1-positive axons from the ventrotemporal region of the retina are repelled by ephrin-B2 at the optic chiasm and adopt the ipsilateral projection path, whereas the vast majority of axons that do not express EphB1 cross the optic chiasm to establish the contralateral projection path (Williams et al., 2003). In *EphB1*$^{-/-}$ and *EphB1*$^{-/-}$ *EphB2*$^{-/-}$*EphB3*$^{-/-}$ mice, ipsilateral projections were decreased by 43 and 56 percent, respectively (Williams et al., 2003). Similarly, we observed a 55 percent decrease in ipsilateral projections in the *Vav2*$^{-/-}$*Vav3*$^{-/-}$ mice, raising the possibility that Vav proteins might play an important role in EphB1-dependent ipsilateral guidance at the optic chiasm. As we observed clear deficits in ephrin-A-induced endocytosis in *Vav2*$^{-/-}$*Vav3*$^{-/-}$ mice, and both ephrin-A and ephrin-B induce Vav2 tyrosine phosphorylation, it is tempting to speculate that the EphB1-positive axons may be defective in ephrin-B-induced endocytosis. If this is the case, then in the *Vav2*$^{-/-}$*Vav3*$^{-/-}$ mice the EphB1-positive axons may bind to the ephrin-B2-positive glia but fail to undergo ephrin-Eph endocytosis and axonal repulsion. In the future, it will be important to test whether Vav proteins regulate ephrin-B-EphB endocytosis and repulsive signaling, as well as to determine the fate of the absent ipsilateral axons in the *Vav2*$^{-/-}$*Vav3*$^{-/-}$ mice.

In contrast to studies of ephrin-A-EphA endocytosis and axonal repulsion, it is not yet clear whether ephrin-B-EphB endocytosis is necessary for repulsive signaling. Although ephrin-B1 can stimulate forward endocytosis in cultured mouse neurons, and ephrin-B-EphB endocytosis is required for cell-cell repulsion when EphB and ephrin-B are ectopically expressed in cultured fibroblasts (Marston et al., 2003; Zimmer et al., 2003), *Xenopus* RGCs can undergo growth cone collapse in the absence of forward ephrin-B-EphB endocytosis (Mann et al., 2003). This suggests that EphB-mediated repulsion can, at least under some circumstances, occur independently of endocytosis. As these studies emphasize, it will be important to determine whether ephrin-B-EphB endocytosis occurs in vivo during normal axon guidance and whether ephrin-B-EphB endocytosis is required for cell-cell detachment and axonal repulsion.

The reduction of projections to the dLGN in the *Vav2*$^{-/-}$*Vav3*$^{-/-}$ mice is not the only observed retinogeniculate targeting defect. The remaining ipsilateral projections along the dorsomedial to VL axis of the dLGN are also abnormally distributed (Figure 5C). In wild-type mice, ephrin-A2 and ephrin-A5 are expressed in a gradient along this axis with highest expression at the VL region (Feldheim et al., 1998). In addition, ephrin-As are critical for RGC axon targeting along this axis. Specifically, *ephrin-A5*$^{-/-}$ and *ephrin-A2*$^{-/-}$*ephrin-A5*$^{-/-}$ mice display mistargeted projections along the plane of the ephrin-A gradient (Feldheim et al., 2000; Feldheim et al., 1998; Frisen et al., 1998). Interestingly, the mistargeted ipsilateral projections in the *Vav2*$^{-/-}$*Vav3*$^{-/-}$ mice were shifted toward the higher concentrations of ephrin-A, raising the possibility that defective endocytosis of the ephrin-A-EphA complex and/or repulsive signaling may result in attraction/adhesion toward more ventrolateral positions (i.e., higher concentrations of ephrin-A) in the dLGN. With our current data, we cannot firmly establish that the shift in ipsilateral projections in Vav-deficient mice represents defective Eph signaling or ephrin-Eph endocytosis; however, the fact that the abnormal axonal projection pattern is specifically defective in the axis of the ephrin-A gradient and that cultured Vav-deficient RGCs are defective in ephrin-A-induced growth cone collapse and endocytosis suggests that Vav proteins may play a critical role in ephrin-A/EphA-dependent repulsion in vivo.

Although there is now considerable evidence suggesting that ephrin-Eph endocytosis plays an important role in repulsive signaling, Flanagan and colleagues have reported that the proteolytic cleavage of the ephrin-A ligand is also required for ephrin-A-induced repulsion (Hattori et al., 2000). Upon ephrin-A-EphA binding, the metalloprotease Kuzbanian (Adam10) cleaves the ephrin-A ligand, thus providing a mechanism for disrupting the ephrin-A-EphA adhesion event. Failure to proteolyze ephrin-A resulted in delayed axonal repulsion, suggesting that ephrin-A cleavage is a critical step for normal repulsive signaling. In the future, it will be important to explore the relationship between the ephrin-A cleavage event and Rac-dependent ephrin-

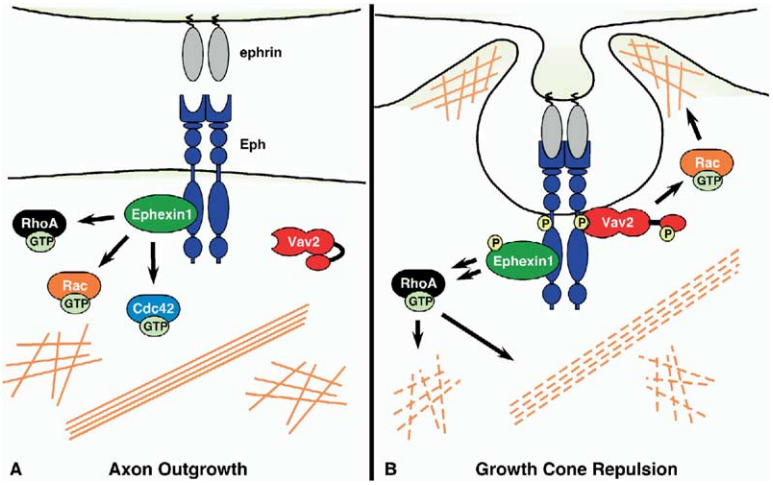

Figure 8. A Model for How Vav and Ephexin Family GEFs May Mediate Axonal Outgrowth and Ephrin-Induced Growth Cone Repulsion

Eph endocytosis during the processes of Eph-mediated axonal repulsion or attraction.

One question that our study raises is how Vav proteins promote ephrin-Eph endocytosis. The growth cone collapse and endocytosis assays demonstrate a requirement for Vav proteins for these processes in cultured neurons, but it is not yet clear how Vav proteins mediate these processes. Since local activation of a Rho family GTPase appears to be necessary for endocytosis, we suspect that the GEF activity of Vav proteins is required for endocytosis and growth cone collapse. In support of this idea, we find that overexpression of a dominant interfering form of Vav2 that lacks GDP/GTP exchange activity reduces the responsiveness of wild-type rat RGCs to ephrin-induced growth cone collapse (C.W.C. and M.S., unpublished data). However, Vav proteins contain a number of additional functional domains (Figure 1C) that may also play a role in Vav-dependent Eph forward signaling.

In addition to understanding the mechanism by which Vav proteins promote ephrin-Eph endocytosis, we are also interested in understanding how this endocytic event induces a repulsive response. Recent studies indicate that the endocytosis of ligand-receptor complexes can determine signaling output. For example, endocytosis and retrograde transport of the activated neurotrophin receptor complex is required for transmission of the survival signal in neurons (Heerssen et al., 2004; Kuruvilla et al., 2004; York et al., 2000; Zhang et al., 2000). Similarly, regulated endocytosis of the epidermal growth factor (EGF) receptor (EGFR) contributes to productive EGF signaling, and dysregulation of EGFR trafficking may contribute to cellular transformation (Levkowitz et al., 1998). For ephrin-Eph endocytosis, it will be interesting to learn whether the recruited factors and signaling outputs are different between surface-localized Ephs and endocytic vesicle-localized Ephs. Furthermore, as Vav proteins have been found to be activated downstream of a number of growth factor receptors such as EGFR and PDGF-R (Liu and Burridge, 2000; Moores et al., 2000; Pandey et al., 2000; Tamas et al., 2003; Tamas et al., 2001), it will be important to examine the role of Vav family GEFs in the ligand-induced endocytosis of other cell surface receptors.

Our findings suggest that Ephs promote repulsion by orchestrating a series of distinct events and that activated Ephs engage different GEFs to affect the distinct actin cytoskeletal changes necessary for repulsion (Figure 8). Specifically, we find that both ephexin1 (Shamah et al., 2001; Sahin et al., 2005) and Vav proteins are necessary for ephrin-A-induced growth cone collapse but that these GEFs appear to regulate distinct aspects of repulsive signaling. Upon ephrin-Eph binding, Vav2 is recruited to the autophosphorylated Eph and becomes rapidly and transiently activated, possibly by Src family kinases (Marignani and Carpenter, 2001; Schuebel et al., 1998), to promote local Rac-dependent endocytosis of the ephrin-Eph complex and surrounding plasma membrane. Similarly, ephexin1 becomes tyrosine phosphorylated, resulting in a strong switch to RhoA activation, which is necessary for F-actin disassembly and contractility. It will be worthwhile to understand the temporal and causal relationship between endocytosis and repulsive signaling that stimulates F-actin contractility and disassembly during Eph-mediated axon guidance. If Rac-dependent endocytosis regulates RhoA-dependent repulsive signaling, then regulation of ephrin-Eph endocytosis could determine whether ephrin-Eph binding promotes attraction/adhesion or repulsion.

Taken together, the findings described here implicate Vav family GEFs as critical regulators of Eph forward signaling in vitro and in vivo. By regulating endocytosis of the ephrin-Eph complex, Vav proteins may convert an initially adhesive interaction of ephrin-Eph binding to repulsive signaling. It remains to be determined whether Vav proteins play more general roles as mediators of endocytic processes and how Vav proteins might mediate these responses.

Experimental Procedures

Yeast Two-Hybrid Screening

Briefly, mouse EphA4 (amino acids 570–986) was screened as bait using an E14 rat spinal cord/DRG cDNA library consisting of 2 ×

10^6 primary transformants as previously described (Shamah et al., 2001).

Antibodies, DNA Constructs, and Coimmunoprecipitations

Details can be found in the Supplemental Data.

Generation of *Vav2*$^{-/-}$*Vav3*$^{-/-}$ Mice

Details can be found in the Supplemental Data.

Analysis of Retinogeniculate Projections

Mouse pups at postnatal day 14 were injected binocularly with fluorescence-labeled Cholera Toxin B subunit (Alexa-488 or Alexa-594; Molecular Probes) and allowed to recover for 36 hr. Dissected brains were fixed in 10% (v/v) formalin for 48 hr at 4°C. Coronal sections (100 μm) were imaged with a Zeiss confocal microscope with a 10× objective. Images were acquired from similar sections under blinded conditions. To normalize images for differences in labeling efficiency, we adjusted the laser intensity such that peak pixel values were just saturating. However, most images had peak values that were nearly identical, allowing for identical settings for imaging and analysis. Contralateral and ipsilateral images were analyzed using NIH ImageJ software. Background subtraction was performed by 200 pixel rolling ball method as described (Torborg and Feller, 2004).

Growth Cone Collapse Assays

Details can be found in the Supplemental Data.

Ephrin-Eph Endocytosis Assays

Cultured RGCs (P6–P7) were incubated with 5 μg/ml ephrin-A1-Fc or Fc control, or 100 μg/ml transferrin (tetramethylrhodamine conjugated; Molecular Probes) for 3–30 min at 37°C or 4°C. Cells were washed three times with ice-cold D-PBS then fixed for 10 min with 4% PFA/2% sucrose in D-PBS at room temperature. For ephrin-A1 endocytosis assays, cells were blocked with 3% (w/v) BSA, 5% (v/v) goat serum, D-PBS in the presence or absence of 0.1% (v/v) Triton X-100. Surface bound (unpermeabilized) or total (detergent permeabilized) ephrin-A1-Fc or Fc control was detected using anti-human Fc conjugated with Cy3 (Jackson Immunoresearch Labs) at 1/300 dilution for 1 hr. Growth cone morphology was visualized using DiO(C_6) (Molecular Probes) at 500 ng/ml in D-PBS for 2–3 min. RGCs were imaged with a 60× oil objective lens using a Nikon (E600) fluorescence microscope. The distal-most 12 microns of RGC neurites were identified by DiO staining and outlined using NIH ImageJ software. Mean pixel intensity of the distal processes in the Cy3 channel was measured and adjusted for local background. For endocytosis of transferrin, RGCs were placed on ice and washed twice with ice-cold D-PBS, twice with ice-cold 500 mM NaCl/0.2N acetic acid solution (5 min incubation for first wash), and then twice with ice-cold PBS to readjust pH to neutral. RGCs were fixed in 4% PFA/2% sucrose in D-PBS at room temperature for 10 min and then stained with DiO. Internalized transferrin-TRITC was imaged and quantified from RGC cell bodies.

Supplemental Data

The Supplemental Data include Supplemental Experimental Procedures and one supplemental figure and can be found with this article online at http://www.neuron.org/cgi/content/full/46/2/205/DC1/.

Acknowledgments

The authors would like to thank Linda Hu for assistance with antibody purification; Louisa Mook and Renatta Knox for technical assistance; Tae-Kyung Kim and Steven Flavell for assistance with developmental expression data; Zhigang He for the gift of Sema3A protein; Rosalind Segal for the DRG explant lysates; Sara Vasquez for technical assistance with neuronal cell cultures; and Ben Barres and Jeff Goldberg for RGC culture protocols. *Vav2*$^{-/-}$ and *Vav3*$^{-/-}$ mice were generous gifts of Martin Turner (Babraham Institute, Cambridge, UK) and Wojciech Swat (Washington University, St. Louis, MO), respectively. M.E.G. acknowledges the generous support of the F.M. Kirby Foundation to the Neurobiology Program of Children's Hospital. This work was supported by a NRSA grant (AG05870) from the National Institute of Aging (C.W.C.); a Lefler Foundation postdoctoral fellowship (C.W.C.); a Fu Foundation predoctoral fellowship (Y.R.S.); National Institute of Child Health and Human Development grant K08 HD01384 (M.S.); a NSF predoctoral fellowship (P.L.G.); NIH grant HL059561 and ACS Research Professorship (J.S.B.); Mental Retardation Research Center grant HD18655 and NIH grant NS43855 (M.E.G.); and a grant from Daiichi Pharmaceuticals (M.E.G.).

Received: October 27, 2004
Revised: February 15, 2005
Accepted: March 22, 2005
Published: April 20, 2005

References

Aghazadeh, B., Lowry, W.E., Huang, X.Y., and Rosen, M.K. (2000). Structural basis for relief of autoinhibition of the Dbl homology domain of proto-oncogene Vav by tyrosine phosphorylation. Cell *102*, 625–633.

Arthur, W.T., Quilliam, L.A., and Cooper, J.A. (2004). Rap1 promotes cell spreading by localizing Rac guanine nucleotide exchange factors. J. Cell Biol. *167*, 111–122.

Bartley, T.D., Hunt, R.W., Welcher, A.A., Boyle, W.J., Parker, V.P., Lindberg, R.A., Lu, H.S., Colombero, A.M., Elliott, R.L., and Guthrie, B.A. (1994). B61 is a ligand for the ECK receptor protein-tyrosine kinase. Nature *368*, 558–560.

Binns, K.L., Taylor, P.P., Sicheri, F., Pawson, T., and Holland, S.J. (2000). Phosphorylation of tyrosine residues in the kinase domain and juxtamembrane region regulates the biological and catalytic activities of Eph receptors. Mol. Cell. Biol. *20*, 4791–4805.

Bustelo, X.R. (2000). Regulatory and signaling properties of the Vav family. Mol. Cell. Biol. *20*, 1461–1477.

Bustelo, X.R. (2001). Vav proteins, adaptors and cell signaling. Oncogene *20*, 6372–6381.

Chauvet, N., Prieto, M., Fabre, C., Noren, N.K., and Privat, A. (2003). Distribution of p120 catenin during rat brain development: potential role in regulation of cadherin-mediated adhesion and actin cytoskeleton organization. Mol. Cell. Neurosci. *22*, 467–486.

Crespo, P., Schuebel, K.E., Ostrom, A.A., Gutkind, J.S., and Bustelo, X.R. (1997). Phosphotyrosine-dependent activation of Rac-1 GDP/GTP exchange by the vav proto-oncogene product. Nature *385*, 169–172.

Davis, A., Sage, C.R., Dougherty, C.A., and Farrell, K.W. (1994). Microtubule dynamics modulated by guanosine triphosphate hydrolysis activity of beta-tubulin. Science *264*, 839–842.

Dearborn, R., Jr., He, Q., Kunes, S., and Dai, Y. (2002). Eph receptor tyrosine kinase-mediated formation of a topographic map in the Drosophila visual system. J. Neurosci. *22*, 1338–1349.

Drescher, U., Kremoser, C., Handwerker, C., Loschinger, J., Noda, M., and Bonhoeffer, F. (1995). In vitro guidance of retinal ganglion cell axons by RAGS, a 25 kDa tectal protein related to ligands for Eph receptor tyrosine kinases. Cell *82*, 359–370.

Ellis, C., Kasmi, F., Ganju, P., Walls, E., Panayotou, G., and Reith, A.D. (1996). A juxtamembrane autophosphorylation site in the Eph family receptor tyrosine kinase, Sek, mediates high affinity interaction with p59fyn. Oncogene *12*, 1727–1736.

Feldheim, D.A., Vanderhaeghen, P., Hansen, M.J., Frisen, J., Lu, Q., Barbacid, M., and Flanagan, J.G. (1998). Topographic guidance labels in a sensory projection to the forebrain. Neuron *21*, 1303–1313.

Feldheim, D.A., Kim, Y.I., Bergemann, A.D., Frisen, J., Barbacid, M., and Flanagan, J.G. (2000). Genetic analysis of ephrin-A2 and ephrin-A5 shows their requirement in multiple aspects of retinocollicular mapping. Neuron *25*, 563–574.

Flanagan, J.G., and Vanderhaeghen, P. (1998). The ephrins and Eph receptors in neural development. Annu. Rev. Neurosci. *21*, 309–345.

Fournier, A.E., Nakamura, F., Kawamoto, S., Goshima, Y., Kalb,

R.G., and Strittmatter, S.M. (2000). Semaphorin3A enhances endocytosis at sites of receptor-F-actin colocalization during growth cone collapse. J. Cell Biol. *149*, 411–422.

Frisen, J., Yates, P.A., McLaughlin, T., Friedman, G.C., O'Leary, D.D., and Barbacid, M. (1998). Ephrin-A5 (AL-1/RAGS) is essential for proper retinal axon guidance and topographic mapping in the mammalian visual system. Neuron *20*, 235–243.

Guan, K.L., and Rao, Y. (2003). Signalling mechanisms mediating neuronal responses to guidance cues. Nat. Rev. Neurosci. *4*, 941–956.

Hattori, M., Osterfield, M., and Flanagan, J.G. (2000). Regulated cleavage of a contact-mediated axon repellent. Science *289*, 1360–1365.

He, Z., and Tessier-Lavigne, M. (1997). Neuropilin is a receptor for the axonal chemorepellent Semaphorin III. Cell *90*, 739–751.

Heerssen, H.M., Pazyra, M.F., and Segal, R.A. (2004). Dynein motors transport activated Trks to promote survival of target-dependent neurons. Nat. Neurosci. *7*, 596–604.

Henkemeyer, M., Itkis, O.S., Ngo, M., Hickmott, P.W., and Ethell, I.M. (2003). Multiple EphB receptor tyrosine kinases shape dendritic spines in the hippocampus. J. Cell Biol. *163*, 1313–1326.

Holland, S.J., Gale, N.W., Gish, G.D., Roth, R.A., Songyang, Z., Cantley, L.C., Henkemeyer, M., Yancopoulos, G.D., and Pawson, T. (1997). Juxtamembrane tyrosine residues couple the Eph family receptor EphB2/Nuk to specific SH2 domain proteins in neuronal cells. EMBO J. *16*, 3877–3888.

Jurney, W.M., Gallo, G., Letourneau, P.C., and McLoon, S.C. (2002). Rac1-mediated endocytosis during ephrin-A2- and semaphorin 3A-induced growth cone collapse. J. Neurosci. *22*, 6019–6028.

Kawakatsu, T., Ogita, H., Fukuhara, T., Fukuyama, T., Minami, Y., Shimizu, K., and Takai, Y. (2005). Vav2 as a Rac-GEF responsible for the nectin-induced, c-Src- and Cdc42-mediated activation of Rac. J. Biol. Chem. *280*, 4940–4947.

Kolodkin, A.L., Matthes, D.J., O'Connor, T.P., Patel, N.H., Admon, A., Bentley, D., and Goodman, C.S. (1992). Fasciclin IV: sequence, expression, and function during growth cone guidance in the grasshopper embryo. Neuron *9*, 831–845.

Kolodkin, A.L., Levengood, D.V., Rowe, E.G., Tai, Y.T., Giger, R.J., and Ginty, D.D. (1997). Neuropilin is a semaphorin III receptor. Cell *90*, 753–762.

Kullander, K., and Klein, R. (2002). Mechanisms and functions of Eph and ephrin signalling. Nat. Rev. Mol. Cell Biol. *3*, 475–486.

Kullander, K., Mather, N.K., Diella, F., Dottori, M., Boyd, A.W., and Klein, R. (2001). Kinase-dependent and kinase-independent functions of EphA4 receptors in major axon tract formation in vivo. Neuron *29*, 73–84.

Kuruvilla, R., Zweifel, L.S., Glebova, N.O., Lonze, B.E., Valdez, G., Ye, H., and Ginty, D.D. (2004). A neurotrophin signaling cascade coordinates sympathetic neuron development through differential control of TrkA trafficking and retrograde signaling. Cell *118*, 243–255.

Levkowitz, G., Waterman, H., Zamir, E., Kam, Z., Oved, S., Langdon, W.Y., Beguinot, L., Geiger, B., and Yarden, Y. (1998). c-Cbl/Sli-1 regulates endocytic sorting and ubiquitination of the epidermal growth factor receptor. Genes Dev. *12*, 3663–3674.

Liu, B.P., and Burridge, K. (2000). Vav2 activates Rac1, Cdc42, and RhoA downstream from growth factor receptors but not beta1 integrins. Mol. Cell. Biol. *20*, 7160–7169.

Lopez-Lago, M., Lee, H., Cruz, C., Movilla, N., and Bustelo, X.R. (2000). Tyrosine phosphorylation mediates both activation and downmodulation of the biological activity of Vav. Mol. Cell. Biol. *20*, 1678–1691.

Luo, Y., Raible, D., and Raper, J.A. (1993). Collapsin: a protein in brain that induces the collapse and paralysis of neuronal growth cones. Cell *75*, 217–227.

Mann, F., Miranda, E., Weinl, C., Harmer, E., and Holt, C.E. (2003). B-type Eph receptors and ephrins induce growth cone collapse through distinct intracellular pathways. J. Neurobiol. *57*, 323–336.

Marcoux, N., and Vuori, K. (2003). EGF receptor mediates adhesion-dependent activation of the Rac GTPase: a role for phosphatidylinositol 3-kinase and Vav2. Oncogene *22*, 6100–6106.

Marignani, P.A., and Carpenter, C.L. (2001). Vav2 is required for cell spreading. J. Cell Biol. *154*, 177–186.

Marston, D.J., Dickinson, S., and Nobes, C.D. (2003). Rac-dependent trans-endocytosis of ephrinBs regulates Eph-ephrin contact repulsion. Nat. Cell Biol. *5*, 879–888.

Meima, L., Kljavin, I.J., Moran, P., Shih, A., Winslow, J.W., and Caras, I.W. (1997a). AL-1-induced growth cone collapse of rat cortical neurons is correlated with REK7 expression and rearrangement of the actin cytoskeleton. Eur. J. Neurosci. *9*, 177–188.

Meima, L., Moran, P., Matthews, W., and Caras, I.W. (1997b). Lerk2 (ephrin-B1) is a collapsing factor for a subset of cortical growth cones and acts by a mechanism different from AL-1 (ephrin-A5). Mol. Cell. Neurosci. *9*, 314–328.

Moores, S.L., Selfors, L.M., Fredericks, J., Breit, T., Fujikawa, K., Alt, F.W., Brugge, J.S., and Swat, W. (2000). Vav family proteins couple to diverse cell surface receptors. Mol. Cell. Biol. *20*, 6364–6373.

Movilla, N., and Bustelo, X.R. (1999). Biological and regulatory properties of Vav-3, a new member of the Vav family of oncoproteins. Mol. Cell. Biol. *19*, 7870–7885.

Pandey, A., Lazar, D.F., Saltiel, A.R., and Dixit, V.M. (1994). Activation of the Eck receptor protein tyrosine kinase stimulates phosphatidylinositol 3-kinase activity. J. Biol. Chem. *269*, 30154–30157.

Pandey, A., Duan, H., and Dixit, V.M. (1995). Characterization of a novel Src-like adapter protein that associates with the Eck receptor tyrosine kinase. J. Biol. Chem. *270*, 19201–19204.

Pandey, A., Podtelejnikov, A.V., Blagoev, B., Bustelo, X.R., Mann, M., and Lodish, H.F. (2000). Analysis of receptor signaling pathways by mass spectrometry: identification of vav-2 as a substrate of the epidermal and platelet-derived growth factor receptors. Proc. Natl. Acad. Sci. USA *97*, 179–184.

Sahin, M., Greer, P.L., Lin, M.Z., Poucher, H., Eberhart, J., Schmidt, S., Wright, T.M., Shamah, S.M., O'Connell, S., Cowan, C.W., et al. (2005). Eph-dependent tyrosine phosphorylation of ephexin1 modulates growth cone collapse. Neuron *46*, this issue, 179–184.

Schuebel, K.E., Movilla, N., Rosa, J.L., and Bustelo, X.R. (1998). Phosphorylation-dependent and constitutive activation of Rho proteins by wild-type and oncogenic Vav-2. EMBO J. *17*, 6608–6621.

Servitja, J.M., Marinissen, M.J., Sodhi, A., Bustelo, X.R., and Gutkind, J.S. (2003). Rac1 function is required for Src-induced transformation. Evidence of a role for Tiam1 and Vav2 in Rac activation by Src. J. Biol. Chem. *278*, 34339–34346.

Shamah, S.M., Lin, M.Z., Goldberg, J.L., Estrach, S., Sahin, M., Hu, L., Bazalakova, M., Neve, R.L., Corfas, G., Debant, A., and Greenberg, M.E. (2001). EphA receptors regulate growth cone dynamics through the novel guanine nucleotide exchange factor ephexin. Cell *105*, 233–244.

Stein, E., Cerretti, D.P., and Daniel, T.O. (1996). Ligand activation of ELK receptor tyrosine kinase promotes its association with Grb10 and Grb2 in vascular endothelial cells. J. Biol. Chem. *271*, 23588–23593.

Stein, E., Huynh-Do, U., Lane, A.A., Cerretti, D.P., and Daniel, T.O. (1998). Nck recruitment to Eph receptor, EphB1/ELK, couples ligand activation to c-Jun kinase. J. Biol. Chem. *273*, 1303–1308.

Takahashi, T., Fournier, A., Nakamura, F., Wang, L.H., Murakami, Y., Kalb, R.G., Fujisawa, H., and Strittmatter, S.M. (1999). Plexin-neuropilin-1 complexes form functional semaphorin-3A receptors. Cell *99*, 59–69.

Tamagnone, L., Artigiani, S., Chen, H., He, Z., Ming, G.I., Song, H., Chedotal, A., Winberg, M.L., Goodman, C.S., Poo, M., et al. (1999). Plexins are a large family of receptors for transmembrane, secreted, and GPI-anchored semaphorins in vertebrates. Cell *99*, 71–80.

Tamas, P., Solti, Z., and Buday, L. (2001). Membrane-targeting is critical for the phosphorylation of Vav2 by activated EGF receptor. Cell. Signal. *13*, 475–481.

Tamas, P., Solti, Z., Bauer, P., Illes, A., Sipeki, S., Bauer, A., Farago,

A., Downward, J., and Buday, L. (2003). Mechanism of epidermal growth factor regulation of Vav2, a guanine nucleotide exchange factor for Rac. J. Biol. Chem. *278*, 5163–5171.

Tessier-Lavigne, M., and Goodman, C.S. (1996). The molecular biology of axon guidance. Science *274*, 1123–1133.

Torborg, C.L., and Feller, M.B. (2004). Unbiased analysis of bulk axonal segregation patterns. J. Neurosci. Methods *135*, 17–26.

Turner, M., and Billadeau, D.D. (2002). VAV proteins as signal integrators for multi-subunit immune-recognition receptors. Nat. Rev. Immunol. *2*, 476–486.

Wahl, S., Barth, H., Ciossek, T., Aktories, K., and Mueller, B.K. (2000). Ephrin-A5 induces collapse of growth cones by activating Rho and Rho kinase. J. Cell Biol. *149*, 263–270.

Walkenhorst, J., Dutting, D., Handwerker, C., Huai, J., Tanaka, H., and Drescher, U. (2000). The EphA4 receptor tyrosine kinase is necessary for the guidance of nasal retinal ganglion cell axons in vitro. Mol. Cell. Neurosci. *16*, 365–375.

Williams, S.E., Mann, F., Erskine, L., Sakurai, T., Wei, S., Rossi, D.J., Gale, N.W., Holt, C.E., Mason, C.A., and Henkemeyer, M. (2003). Ephrin-B2 and EphB1 mediate retinal axon divergence at the optic chiasm. Neuron *39*, 919–935.

York, R.D., Molliver, D.C., Grewal, S.S., Stenberg, P.E., McCleskey, E.W., and Stork, P.J. (2000). Role of phosphoinositide 3-kinase and endocytosis in nerve growth factor-induced extracellular signal-regulated kinase activation via Ras and Rap1. Mol. Cell. Biol. *20*, 8069–8083.

Zhang, Y., Moheban, D.B., Conway, B.R., Bhattacharyya, A., and Segal, R.A. (2000). Cell surface Trk receptors mediate NGF-induced survival while internalized receptors regulate NGF-induced differentiation. J. Neurosci. *20*, 5671–5678.

Zimmer, M., Palmer, A., Kohler, J., and Klein, R. (2003). EphB-ephrinB bi-directional endocytosis terminates adhesion allowing contact mediated repulsion. Nat. Cell Biol. *5*, 869–878.

Zisch, A.H., Kalo, M.S., Chong, L.D., and Pasquale, E.B. (1998). Complex formation between EphB2 and Src requires phosphorylation of tyrosine 611 in the EphB2 juxtamembrane region. Oncogene *16*, 2657–2670.

Zisch, A.H., Pazzagli, C., Freeman, A.L., Schneller, M., Hadman, M., Smith, J.W., Ruoslahti, E., and Pasquale, E.B. (2000). Replacing two conserved tyrosines of the EphB2 receptor with glutamic acid prevents binding of SH2 domains without abrogating kinase activity and biological responses. Oncogene *19*, 177–187.